

# **Amidoxime-functionalized Macroporous Carbon Self-Refreshed Electrode Materials for Rapid and High-capacity Removal of Heavy Metal from Water**

Tong Wu<sup>1</sup>, Chong Liu<sup>1</sup>, Biao Kong<sup>1</sup>, Jie Sun<sup>1</sup>, Yongji Gong<sup>1</sup>, Kai Liu<sup>1</sup>, Jin Xie<sup>1</sup>, Allen Pei<sup>1</sup>, Yi Cui<sup>1,2\*</sup>

1. Department of Materials Science and Engineering, Stanford University, Stanford, California 94305, United States.

2. Stanford Institute for Materials and Energy Sciences, SLAC National Accelerator Laboratory, 2575 Sand Hill Road, Menlo Park, California 94305, United States.

*\*Correspondence should be addressed to Y.C. (yicui@stanford.edu).*

Figure S1. The demo of the filtration device.

Figure S2. SEM image of carbon fiber after coating and reaction.

Figure S3. The hydrophilia comparison between three different materials.

Figure S4. The electrical impedances of CF and coated CF.

Figure S5. Flow test of  $\text{Hg}^{2+}$  removal.

Figure S6. Capacity tests and optimization tests of PACCF

Figure S7. EDX images of the deposit on the boundary between polymer coated area and blank area.

Figure S8. Characterization of the deposit sediment.

Figure S9. The SEM images of the deposition after long-term treatment.

Figure S10. Removal and recovery of high concentration heavy metals step by step with AC-DC method.

Note 1. Cost Analysis

Table S1. DFT calculation of binding energy on metals.

Table S2. Performance comparison of other methods before with ours

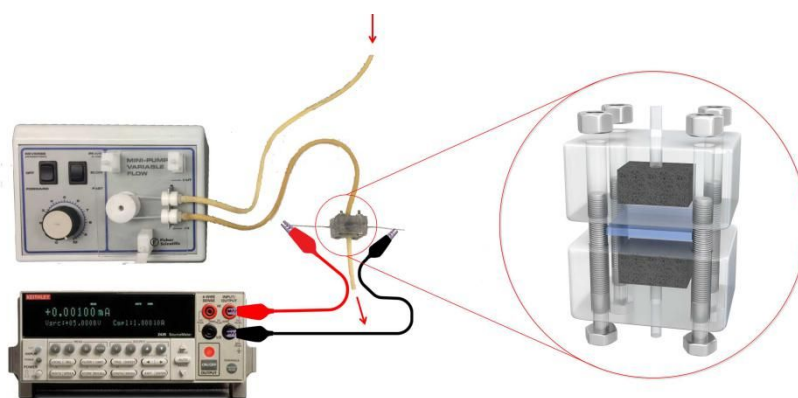


Figure S1. The demo of the filtration device setup and the detail. The kiethley instrument provide the voltage on the cell-filtration device. The peristaltic pump controls the contaminated water loading rate.

The way to get the activated materials mass loading is according to this formula:

$$M = M_3 - M_1 - (M_2 - M_1) / 2$$

$M_1$  is the weight of carbon felt.  $M_2$  is the weight after coated slurry (Super P and PAN).  $M_3$  is the weight after reaction.

Then we can get the capacity of this polymer:

$$E = (C_0 - C_x) \times V / M$$

$C_0$  is the concentration of the original contaminated water.  $C_x$  is the concentration after deposition at that time.  $V$  means the current volume in the container. So that we can realize the filtration capability clearly from the curve in the Figure S2.

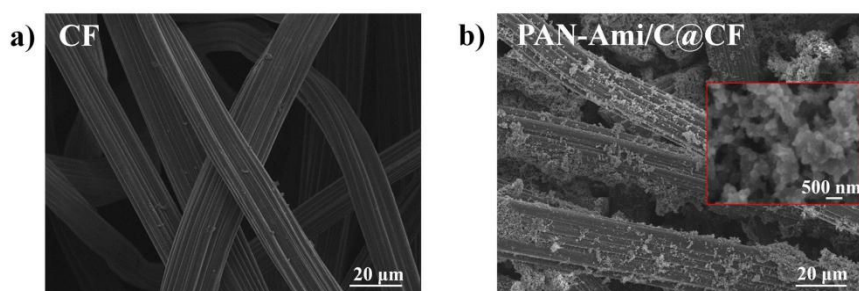


Figure S2. SEM image of carbon fiber. a) Commercial carbon felt. b), PAN-Ami/C coated carbon felt. The insert image shows the ~50nm carbon black nano particles are bound on the fiber surface with help of polymer film.

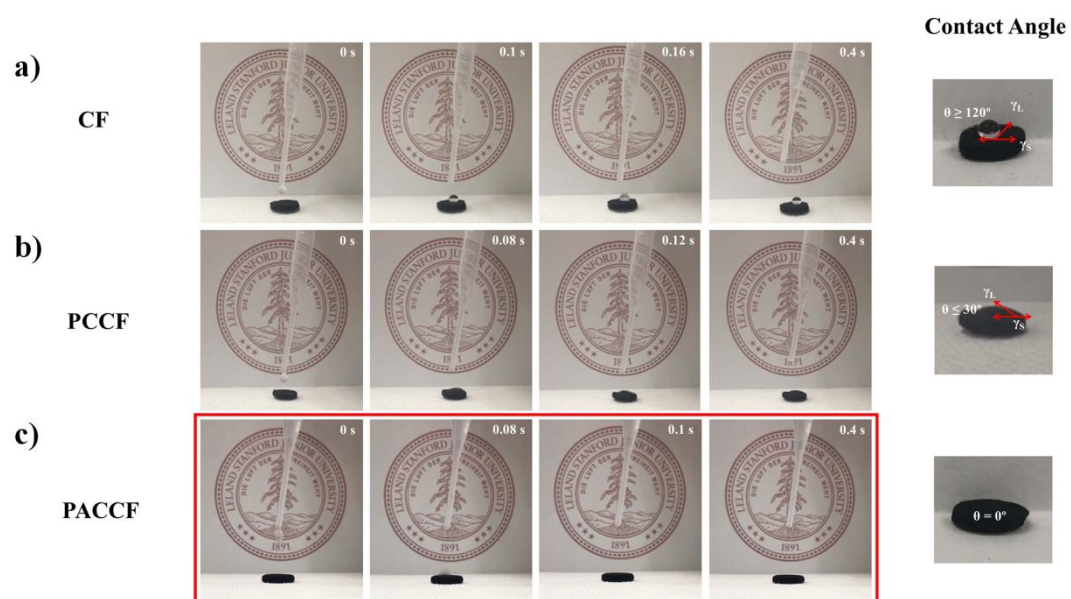


Figure S3. The hydrophilicity comparison between three different materials. a) Commercial CF, the contact angle is over  $120^\circ$ . b) PCCF, the contact angle is less than  $30^\circ$ . c) PACCF. the droplet instantly soaked into the material.

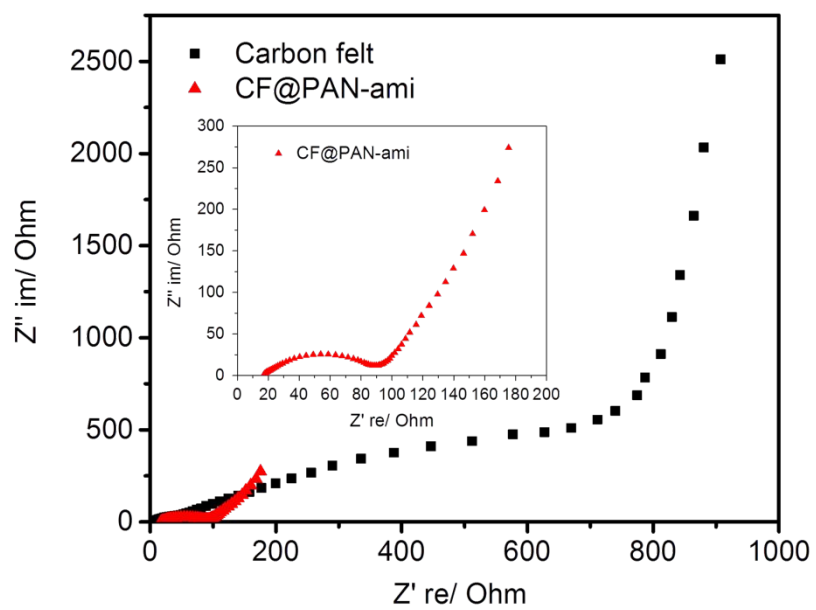


Figure S4. The electrical impedances of CF and coated CF. The black dots are the CF, the red dots are PACCF. All the tests used 0.1 M  $\text{Na}_2\text{SO}_4$  as electrolyte.

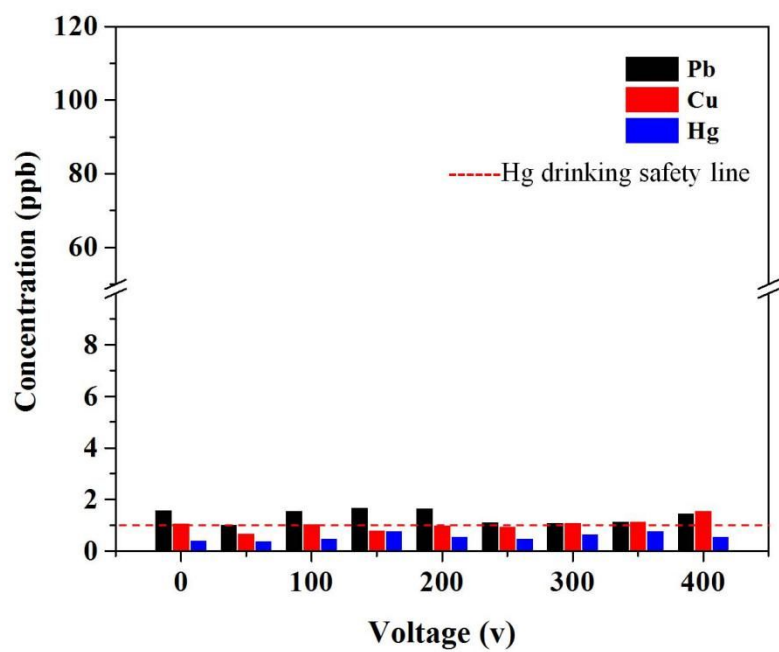


Figure S5. Flow test of  $\text{Hg}^{2+}$  removal under long term running.

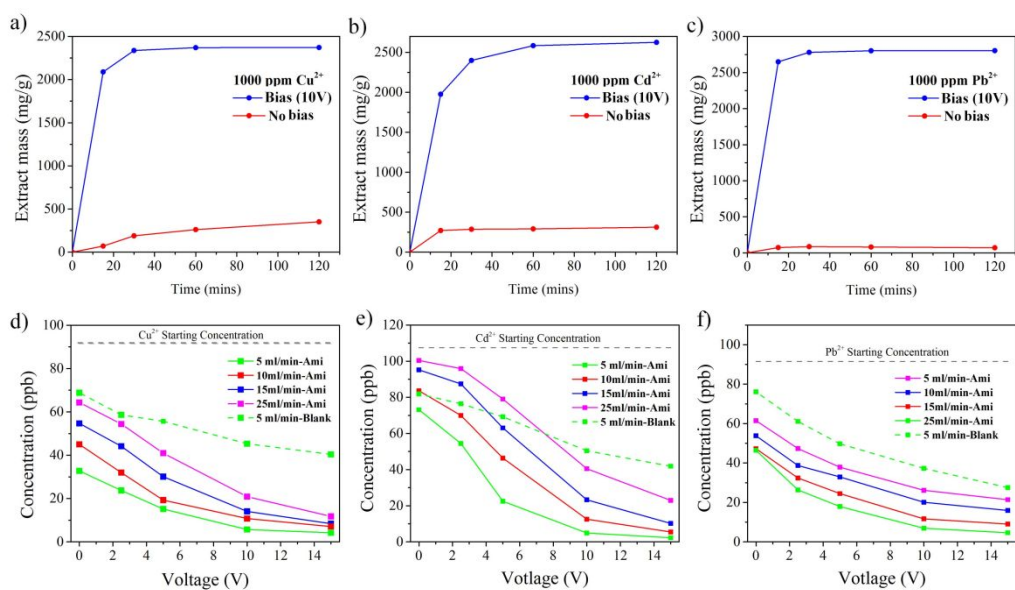


Figure S6. a), b) and c) are capacity tests of PACCF under bias and no bias in the stirring system dealing with 1000 ppm Pb<sup>2+</sup>, Cd<sup>2+</sup>, Cu<sup>2+</sup> contaminated water, respectively (The electrode size is 1 cm<sup>2</sup> × 3.18 cm. The polymer loading weights are 5.9 mg, 5.5 mg and 5.8 mg.). d), e) and f) are optimization tests of 100ppb single-ion simulated water by the flowing device dealing with 100 ppb Pb<sup>2+</sup>, Cd<sup>2+</sup>, Cu<sup>2+</sup> contaminated water, respectively. The red dashes show the safe levels for each cation.



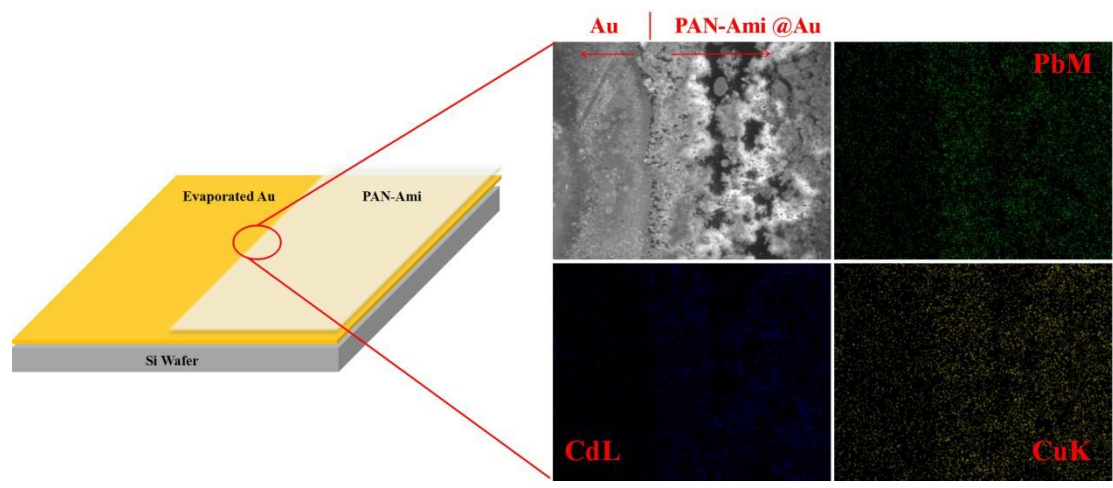


Figure S7. EDX images of the deposit on the boundary between polymer coated area and blank area under 10 V.

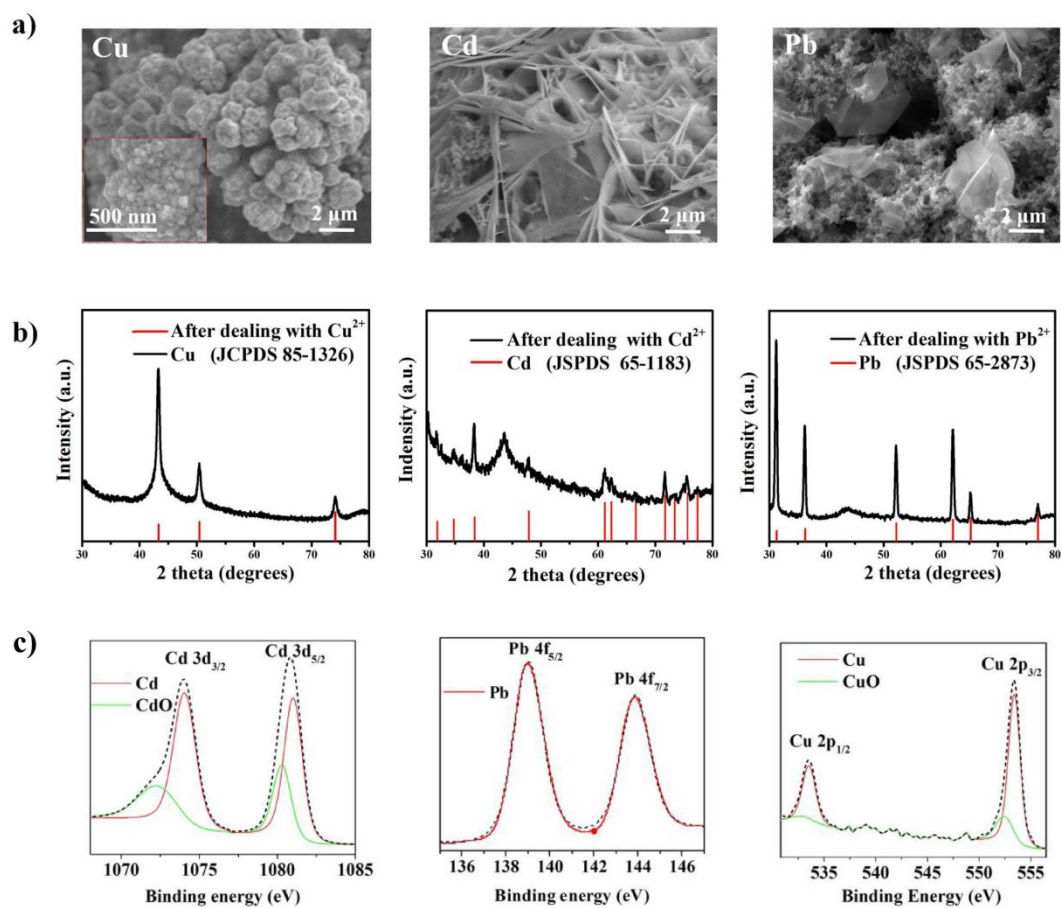


Figure S8. The removal for stirring system with 1000 ppm of single element ( $\text{Cu}^{2+}$ ,  $\text{Cd}^{2+}$ ,  $\text{Pb}^{2+}$ ) simulated water. Each concentration of residue is under the drinking safety level. a) The SEM of these three kinds of deposition covered on the electrodes after 5 min. The inset SEM of Cu shows their assembling cubic structure. b) The XRD of the deposition according to the samples in a) respectively. c) The XPS of the deposition according to the samples in a) respectively.

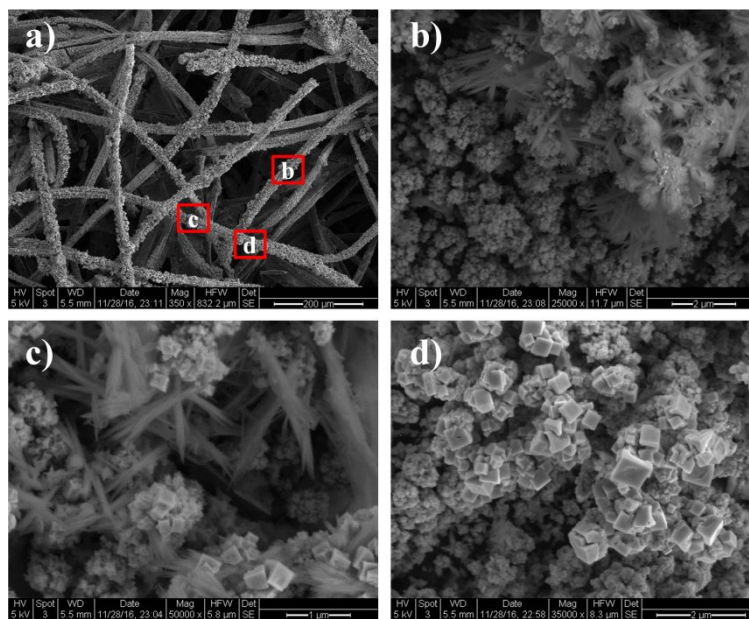


Figure S9. The removal for long term flowing with single element ( $\text{Cu}^{2+}$ ,  $\text{Cd}^{2+}$ ,  $\text{Pb}^{2+}$ ) simulated water. a) The SEM of depositions on the fibers after filtrating 3 days. Respectively, b), c), d) figures show the different nanostructures of heavy metals located on three areas, like cubic structure of Cu and flower-like flake shapes of Cd and Pb.

As we know, each metal ion has its own reduction potential in the same electrochemical working condition. These potential gaps can be used to separate the different metal. So this attempt had been applied in large concentration contaminated water (1000 ppm). In such high concentration, using alternating current instead of direct current can limit the hydrogen evolution and prevent all the ions deposit as hydroxide. Here square-wave alternating current had been applied in 100 Hz. Their reduction potentials are +0.34V ( $\text{Cu}^{2+}/\text{Cu}$ ),  $-0.13\text{ V}$  ( $\text{Pb}^{2+}/\text{Pb}$ ) and  $-0.40\text{ V}$  ( $\text{Cd}^{2+}/\text{Cd}$ ) versus SHE (pH=0), respectively. The pH of our simulated water was around 6, so that the reduction potential of hydrogen here was around  $-0.35\text{ V}$  according to the Nernst equation. Theoretically, the metal ions can be taken out one by one under step-up voltage. But in real experiment, the Cu and Pb were always taken out together. Then the strategy changed the Pb and Cu ions were extracted first as metal in a low voltage (+3.3 V), and switch to the high voltage (1.2 V) to oxidize the Pb (to form  $\text{PbO}_2$ ) and solve the Cu. After 5 hours, over 99% Pb ions had been taken out alone. ( $-0\text{ V}$ ,  $4.2\text{ V}$ ) voltage was applied to attract the Cu ions, after another 5 hours operation, over 99% Cu had been deposit and less than 1% Cd ions left in the mother solution. For the remaining Cd ions, 5 V of DC was applied to rapidly collect them in 2 hours. This direct separation and recovery of heavy metal ions has great value on resources recycling comparing with traditional treatments.

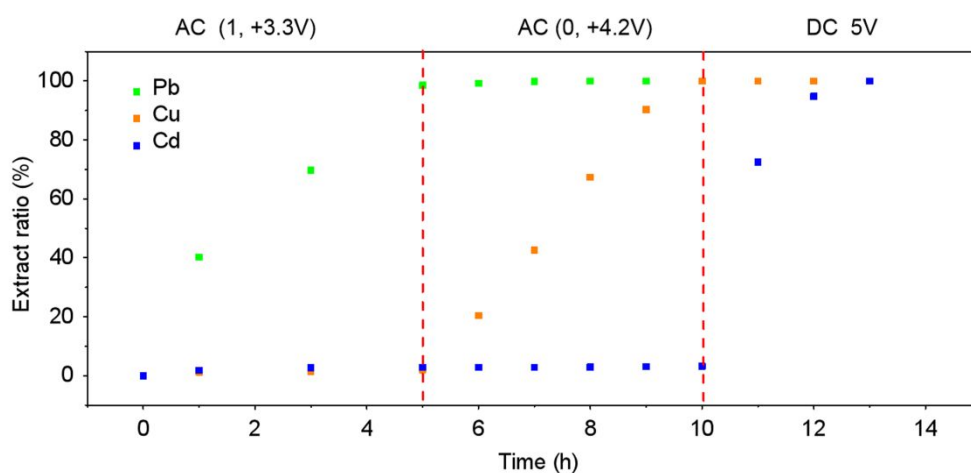


Figure S10. First, AC (1, +3.3V) applied, the Pb ions were removed by 99.99%. Then AC (0, +4.2V) applied, the Cu ions were removed by 99.99%. Last step, 5V of DC applied, the Cd ions were taken out nearly 99.99% (Origin mixture water contained 1000 ppm of  $\text{Cu}^{2+}$ ,  $\text{Cd}^{2+}$ ,  $\text{Pb}^{2+}$  ions each, the frequency of AC was 100 Hz).

**Note 1. Power Consumption Analysis:**

Unlike other pollutants adsorbents,<sup>1-16</sup> the energy consumption mainly generated by applying direct current on the device. So it's necessary to summarize the rough number of cost which can prove it worth to use or not.

The price of electricity used was 4~10 ¢ /kWh in most area of US.

Highest cost:

$$C_{\max} = \$ 0.10 \times 10^{-3} \times V \times I_{\max} \times 1 \text{ h} \times 1000 \text{ kg} / 0.3 \text{ kg} = \$ 6.67 \times 10^{-3}$$

Lowest cost:

$$C_{\min} = \$ 0.04 \times 10^{-3} \times V \times I_{\min} \times 1 \text{ h} \times 1000 \text{ kg} / 0.3 \text{ kg} = \$ 1.33 \times 10^{-3}$$

In the flow device tests with a small piece of materials (1 cm<sup>2</sup>×3.18 cm), the voltage used was 10 V. In one hour, it could deal with 300 ml contaminated water (0.3 kg). The current showed was 1~2 mA. So we can get the maximum and minimum cost according to the formula above. The price of electricity in different state can really change the cost a lot. But the base line of electric charge were extremely low.

**Table S1.**DFT calculation of binding energy between metals and different monomers.<sup>a</sup>

	Cu <sup>2+</sup> (eV)	Cd <sup>2+</sup> (eV)	Pb <sup>2+</sup> (eV)
Amidoxime	66.81	61.96	59.61
Nitrile	6.74	16.56	12.94
Acylamino	9.09	8.14	6.32
Fluoride	11.30	6.30	5.56

<sup>a</sup> Values are calculated based on coordination modes reported before.

**Table S2.**

Performance comparison of other methods before with ours.

Adsorbents	Capacity			Efficiency (Initial C <sub>0</sub> )			Current density A/m <sup>2</sup>	Flow rate L/h	PH	Ref.
	mg/g			% (ppm)						
	Cu	Cd	Pb	Cu	Cd	Pb				
Electroextraction with resins		1.8			>87.5 (40)		2	0.09	-	17
Palm shell activated carbon	7.1	-	23.1	88.8 (50)	-	96.8 (50)	0.1	0.5	5	18
LMOF-263	-	7.0	18.7	-	30 (10)	80 (10)	-	-	-	19
Fe <sub>3</sub> O <sub>4</sub> /HA	46.3	50.4	92.4		> 95 (0.1)		-	-	6	20
Lime and Na <sub>2</sub> S		-		-	95	-	-	-	8.5	21
Few-layered GO nanosheets/HA	-	163	-	-	50	-	-	-	6	22
Graphene-c-MWCNT hybrid aerogel	33.8	-	104.9	-	-	-	-	-	-	23
Electric driven 3D-GMOs	3820	882	434		> 96.0 (100)		-	-	2	24
Electrospun APAN nanofiber mats	150.6	-	60.6	90.5 (200)	-	97.0 (200)	-	-	4	25
This work	2300	2600	2800		> 99.9 (1000)		-	-	6	-
					> 95.0 (0.1)		0.001	0.3		

Reference:

- (1) Mohammadi, N.; Khani, H.; Gupta, V. K.; Amereh, E.; Agarwal, S. Adsorption process of methyl orange dye onto mesoporous carbon material-kinetic and thermodynamic studies. *J. Colloid Interface Sci.* **2011**, *362*, 457-462.
- (2) Rajendran, S.; Khan, M. M.; Gracia, F.; Qin, J. Q.; Gupta, V. K.; Arumainathan, S. Ce<sup>3+</sup>-ion-induced visible-light photocatalytic degradation and electrochemical activity of ZnO/CeO<sub>2</sub> nanocomposite. *Sci. Rep.* **2016**, *6*, 31641.
- (3) Saravanan, R.; Gupta, V. K.; Narayanan, V.; Stephen, A. Comparative study on photocatalytic activity of ZnO prepared by different methods. *J. Mol. Liq.* **2013**, *181*, 133-141.
- (4) Saravanan, R.; Sacari, E.; Gracia, F.; Khan, M. M.; Mosquera, E.; Gupta, V. K. Conducting PANI stimulated ZnO system for visible light photocatalytic degradation of coloured dyes. *J. Mol. Liq.* **2016**, *221*, 1029-1033.
- (5) Saravanan, R.; Karthikeyan, S.; Gupta, V. K.; Sekaran, G.; Narayanan, V.; Stephen, A. Enhanced photocatalytic activity of ZnO/CuO nanocomposite for the degradation of textile dye on visible light illumination. *Mater. Sci. Eng., C* **2013**, *33*, 91-98.
- (6) Devaraj, M.; Saravanan, R.; Deivasigamani, R. K.; Gupta, V. K.; Gracia, F.; Jayadevan, S. Fabrication of novel shape Cu and Cu/Cu<sub>2</sub>O nanoparticles modified electrode for the determination of dopamine and paracetamol. *J. Mol. Liq.* **2016**, *221*, 930-941.
- (7) Saleh, T. A.; Gupta, V. K. Functionalization of tungsten oxide into MWCNT and its application for sunlight-induced degradation of rhodamine B. *J. Colloid Interface Sci.* **2011**, *362*, 337-344.
- (8) Ghaedi, M.; Hajjati, S.; Mahmudi, Z.; Tyagi, I.; Agarwal, S.; Maity, A.; Gupta, V. K.



Modeling of competitive ultrasonic assisted removal of the dyes-Methylene blue and Safranin-O using Fe<sub>3</sub>O<sub>4</sub> nanoparticles. *Chem. Eng. J.* **2015**, *268*, 28-37.

(9) Saleh, T. A.; Gupta, V. K. Photo-catalyzed degradation of hazardous dye methyl orange by use of a composite catalyst consisting of multi-walled carbon nanotubes and titanium dioxide. *J. Colloid Interface Sci.* **2012**, *371*, 101-106.

(10) Gupta, V. K.; Nayak, A.; Agarwal, S.; Tyagi, I. Potential of activated carbon from waste rubber tire for the adsorption of phenolics: Effect of pre-treatment conditions. *J. Colloid Interface Sci.* **2014**, *417*, 420-430.

(11) Mittal, A.; Mittal, J.; Malviya, A.; Gupta, V. K. Removal and recovery of Chrysoidine Y from aqueous solutions by waste materials. *J. Colloid Interface Sci.* **2010**, *344*, 497-507.

(12) Gupta, V. K.; Jain, C. K.; Ali, I.; Chandra, S.; Agarwal, S. Removal of lindane and malathion from wastewater using bagasse fly ash--a sugar industry waste. *Water Res.* **2002**, *36*, 2483-2490.

(13) Gupta, V. K.; Jain, R.; Nayak, A.; Agarwal, S.; Shrivastava, M. Removal of the hazardous dye-tartrazine by photodegradation on titanium dioxide surface. *Mater. Sci. Eng., C* **2011**, *31*, 1062-1067.

(14) Saravanan, R.; Joicy, S.; Gupta, V.; Narayanan, V.; Stephen, A. Visible light induced degradation of methylene blue using CeO<sub>2</sub>/V<sub>2</sub>O<sub>5</sub> and CeO<sub>2</sub>/CuO catalysts. *Mater. Sci. Eng., C* **2013**, *33*, 4725-4731.

(15) Saravanan, R.; Karthikeyan, N.; Gupta, V.; Thirumal, E.; Thangadurai, P.; Narayanan, V.; Stephen, A. ZnO/Ag nanocomposite: an efficient catalyst for degradation studies of textile effluents under visible light. *Mater. Sci. Eng., C* **2013**, *33*, 2235-2244.

(16) Saravanan, R.; Khan, M. M.; Gupta, V. K.; Mosquera, E.; Gracia, F.; Narayanan, V.; Stephen,

A. ZnO/Ag/CdO nanocomposite for visible light-induced photocatalytic degradation of industrial textile effluents. *J. Colloid Interface Sci.* **2015**, *452*, 126-133.

(17) Smara, A.; Delimi, R.; Poinsignon, C.; Sandeaux, J. Electroextraction of heavy metals from diluted solutions by a process combining ionexchange resins and membranes. *Sep. Purif. Technol.* **2005**, *44*, 271-277.

(18) Issabayeva, G.; Aroua, M. K.; Sulaiman, N. M. Electrodeposition of copper and lead on palm shell activated carbon in a flow-through electrolytic cell. *Desalination* **2006**, *194*, 192-201.

(19) Rudd, N. D.; Wang, H.; Fuentes-Fernandez, E. M. A.; Teat, S. J.; Chen, F.; Hall, G.; Chabal, Y. J.; Li, J. Highly efficient luminescent metal-organic framework for the simultaneous detection and removal of heavy metals from water. *ACS Appl. Mater. Interfaces* **2016**, *8*, 30294-30303.

(20) Liu, J.; Zhao, Z.; Jiang, G. Coating Fe<sub>3</sub>O<sub>4</sub> magnetic nanoparticles with humic acid for high efficient removal of heavy metals in water. *Environ. Sci. Technol.* **2008**, *42*, 6949-6954.

(21) Charentanyarak, L. Heavy metals removal by chemical coagulation and precipitation. *Water Sci. Technol.* **1999**, *39*, 135-138.

(22) Zhao, G; Li, J; Ren, X; Chen, C; Wang, X. Few-layered graphene oxide nanosheets as superior sorbents for heavy metal ion pollution management. *Environ. Sci. Technol.* **2011**, *45*, 10454-10462.

(23) Sui, Z. Y.; Meng, Q. H.; Zhang, X. T.; Ma, R.; Cao, B. Green synthesis of carbon nanotube-graphene hybrid aerogels and their use as versatile agents for water purification. *J. Mater. Chem.* **2012**, *22*, 8767-8771.

(24) Li, W.; Gao, S.; Wu, L.; Qiu, S.; Guo, Y.; Geng, X.; Chen, M.; Liao, S.; Zhu, C.; Gong, Y.; Long, M.; Xu, J.; Wei, X.; Sun, M.; Liu, L. High-density three-dimension graphene macroscopic

objects for high-capacity removal of heavy metal ions. *Sci. Rep.* **2013**, *3*, 2125-2130.

(25) Kampalanonwat, P.; Supaphol, P. Preparation and adsorption behavior of aminated electrospun polyacrylonitrile nanofiber mats for heavy metal ion removal. *ACS Appl. Mater. Interfaces* **2010**, *2*, 3619-3627.